Nucleation Theory: A Literature Review and Applications to Nucleation Rates of Natural Gas Hydrates

Simon Davies

SUMMARY

Predicting the onset of hydrate nucleation in oil pipelines is one of the most challenging aspects in the flow assurance modelling work being performed at the Center for Hydrate Research. Nucleation is initiated by a random fluctuation which is able to overcome the energy barrier for the phase transition, once such a fluctuation occurs, further growth is energetically favourable. Historically the random fluctuation requires for nucleation was defined as the formation of a nucleus of critical size. Recently, more realistic models have been proposed based on density functional theory.

In this report, a literature survey of nucleation theory was performed in order to determine the state-of-the-art understanding of hydrate nucleation. A simplified nucleation model was then designed based on a two dimensional Ising model, in order to determine thermodynamic properties for nuclei of various sizes. The model used window sampling to collect high resolution statistics for the high energy states. It was demonstrated that the shape and height of the energy barrier can be determined for a nucleating system in this way.

INTRODUCTION

The ability to predict the onset of nucleation is important for a wide variety of first order phase transitions from industrial crystallisers to rainfall. Systems can be held in a supersaturated state for significant periods of time before a phase transition occurs: distilled water can be held indefinitely at -10ºC without freezing, with further purification it can be cooled to -30ºC without freezing [1]. Predicting the onset of hydrate nucleation in oil pipelines is one of the most challenging aspects in the flow assurance modelling work being performed at the Center for Hydrate Research.

The rate of homogeneous nucleation is determined by the rate of formation of nuclei which maximise the free energy with respect to a property such as radius. After a nucleus reaches this point, further growth becomes energetically favourable. For a single component system, this maximum in free energy arises from the contributions from the surface and the bulk contributions. As more of the system converts to the thermodynamically stable phase, the energy associated with the surface of the nucleus increases in proportion to the radius squared, but the energy of the bulk decreases proportionally to the radius cubed. A random fluctuation is required to overcome the energy barrier; the probability of this fluctuation occurring increases as the driving force for the phase transition increases.

In the case of heterogeneous nucleation, an additional material is added to the system which acts as a catalyst for the phase transition, lowering the energy barrier and increasing the rate of the phase transition. The additional material will have a lower interfacial energy with the new phase than the interface between the two pure phases, meaning that the new phase can form against this material at a lower cost in surface energy. Cracks and defects in the materials surface can increase the phase transition rate further since the filling of these cracks can decrease the surface energy.

In a system with high shear, secondary nucleation can occur where fragments of a nucleus which are themselves above the critical size can be formed, leading to nucleation elsewhere in the system. Fracture pieces are produced more easily from faster growing crystals [2]. The survival of the fracture pieces depends on the supersaturation of the system [3]. There is a maximum rate of nuclei production from fracturing of an existing crystal since the parent crystal needs time to recover [4].

LITERATURE REVIEW

Classical Nucleation Theory

Classical nucleation theory originated in the 1930s and is largely attributed to work by Becker, Döring and Volmer [5]-[6]. The classical approach uses the capillarity approximation, i.e. it assumes that the critical nucleus size is defined as the maximum in the nucleus energy with radius where the energy is calculated as sum of the surface and volume terms which are partitioned. The theory assumes that macroscopic properties can be used for the energy per unit volume of the new phase and that the interfacial energy of a flat surface can be used for the energy of the surface.

In the classical approach, the energy of a critical nucleus of radius R is given by Equation 1 where ΔF_v is the difference in free energy per unit volume between the phases and γ is the interfacial energy per unit area between the phases.

$$E = -\frac{4}{3}\pi R^3 \Delta F_v + 4\pi R^2 \gamma \qquad \text{Equation 1}$$

The height of the energy barrier (E_c^{hom}), shown in Equation 2, can be determined by substituting the expression for the critical radius into Equation 1 where the critical radius (r_c^{hom}) in Equation 3 is deterined by setting the setting the first derivative with radius of Equation 1 to zero [7].

$$E_c^{\,hom} = \frac{16\pi}{3}\frac{\gamma^3}{\left|\Delta F_v\right|^2} \qquad \text{Equation 2} \qquad\qquad r_c^{\,hom} = \frac{2\gamma}{\left|\Delta F_v\right|} \qquad \text{Equation 3}$$

According to the Arrhenius equation, the classical nucleation rate is therefore given by Equation 4 [1].

$$J = J_0 e^{\frac{16\pi\gamma^3}{3|\Delta F_v|^2}}$$ Equation 4

In situations where the size of the critical nucleus is very small (often 20-50 molecules), or the molecules are polar, the classical nucleation approach fails. In these cases, the sharp curvature of the surface will have a significant effect on the interfacial energy, and the structure and corresponding energy of the nucleus may be significantly different from the bulk of the new phase [8]. The most widely applied advancement to the classical approach has been the use of Density Functional Theory [1]. The density functional approach assumes that the free energy of the nucleus ΔF_v depends on the average spherical density profile $\rho(r)$ rather than just the radius.

Density Functional Approach to Nucleation

It is now understood that the density of the new phase at the centre of the nucleus may not be the same as that in the bulk of the new phase [1]. It is proposed instead that spontaneous fluctuations will cause clusters of molecules to arrange themselves in various configurations until they reach a critical density profile $\rho^*(r)$ [9]. Once such a cluster is formed further growth of the new phase is energetically favourable. The critical density profile is the saddle point separating small clusters that tend to shrink from large clusters that tend to grow [1]. The location of the saddle point can be determined by setting the first derivative of the free energy with respect to radius to zero and solving the equation set iteratively.

In order to determine the dependence of the free energy of the cluster on its density profile, a theory is needed to determine the free energy of a non-homogeneous fluid. One such method is the liquid state perturbation theory in which the free energy is calculated from attractive and repulsive contributions to the spherical potential (Equation 5). The repulsive contributions are approximated as the short range repulsions between hard spheres $f_{hs}(\rho(r))$, and attractive contributions $V_{att}(r)$ are approximated from the long range Weeks-Chandler-Anderson[10] approach for separation in simple liquids using either the Lennard-Jones, or in some cases, the less accurate Yukawa [11] potential.

$$E[\rho(r)] = \int dr f_{hs}(\rho(r)) + \iint dr dr' V_{att}(|r - r'|)\rho(r)\rho(r')$$ Equation 5

Effects of Surface Curvature

The surface curvature of small nuclei has a large effect on their interfacial energy which can make cluster formation more energetically favourable in supersaturated solutions [12].The effect is important when the nucleus radius is of the same order of magnitude as the interfacial thickness. The change in interfacial energy is given by Equation 6 [13] where μ is the chemical potential of the bulk fluid, δ is the thickness of the interface and ρ are the densities of the two phases.

$$d\gamma = -\delta(\rho_1 - \rho_2)d\mu \qquad \text{Equation 6}$$

Experimental Validation

In early experimental investigations, such as studies of the nucleation rate of ice, the nucleation rate was calculated from observation of liquid droplets [14] or by measuring the critical nucleation rate where the rate of the phase transition becomes very fast. Recently tools have become available to measure nucleation rates directly such as neutron diffraction [30].

For gas to liquid transitions, non-polar fluids can be modelled fairly well with classical nucleation theory [1]. However, the variation of nucleation rate with temperature is not accounted for properly; theory overpredicts nucleation rates at high temperatures and under predicts at low temperatures [15]. For polar fluids and for multicomponent systems, the classical approach is insufficient. The density functional approach works for weakly polar fluids and helps to explain the trends of nucleation rate with temperature of non-polar fluids [1].

For liquid to solid transitions the behaviour is more complex. The density profile can be periodic for some crystal structures and must be represented by a Fourier series using lattice vectors [16]. There is no spinodal line at which the nucleation barrier vanishes, and sometimes glass transitions occur, at which point the nucleation rate slows down for kinetic reasons [1]. In some systems a metastable phase may form at the interface, lowering the energy barrier for nucleation. One known example of this effect is in the crystallisation of argon-like Lennard Jones fluids where it has been observed that for small critical nuclei, a basic centre cubic structure will form at the centre of the nucleus which evolves to face centre cubic as the nucleus grows larger [17].

Heterogeneous Nucleation

In heterogeneous nucleation, an additional material is added to the system which acts as a catalyst for the phase transition, lowering the energy barrier and increasing the rate of the phase transition. The additional material will have a lower interfacial energy with the new phase than the interface between the two pure phases, meaning that the new phase can form against this material at a lower cost in surface energy. Cracks and defects in the materials surface can increase the phase transition rate further since the filling of these cracks can decrease the surface energy.

The added phase can either be a solid or a liquid, for example it is known that the nucleation point of ice can be lowered by monolayers of aliphatic alcohols ($C_nH_{2n+1}OH$; $16<n<31$) on the surface of water [18]. Silver iodide is known to be a good nucleating agent for clathrate hydrates; it lowers the energy barrier for nucleation, allowing it to nucleate with less subcooling, but does not affect the width of the nucleation distribution [19].

For homogeneous nucleation the height of the energy barrier is defined by Equation 2. In the case of heterogeneous nucleation on a flat surface, the expression is modified by a factor $f^{het}(\theta)$ [7] as shown in Equation 6 and 7 where θ is the contact angle between the nucleus and the extrinsic object. For a spherical surface of radius R, the energy is given by Equation 8 [7] where φ is the angle at the centre of the sphere between the centre and the edge of the nucleus (radius r).

$$E_c^{het} = \frac{16\pi}{3}\frac{\gamma^3}{\left|\Delta F_v\right|^2} f^{het}(\theta) \quad \text{Equation 6} \qquad f^{het}(\theta) = \frac{2-3\cos\theta+\cos^3\theta}{4} \quad \text{Equation 7}$$

$$E_c^{het} = 2\pi\gamma r^2\left[1-\cos(\theta+\varphi)\right] - 2\pi\gamma R^2\cos\theta(1-\cos\varphi) - \frac{\pi}{3}r^3\Delta F_v\left[2-3\cos(\theta+\varphi)+\cos^3(\theta+\varphi)\right] + \frac{\pi}{3}\Delta F_v R^3\left[2-3\cos(\varphi)+\cos^3(\varphi)\right]$$

Equation 8

Hydrate Nucleation Theories

Clathrate hydrates are crystalline inclusion compounds that consist of a hydrogen bonded lattice comprised of water cages which encapsulate small gas molecules at high pressures and low temperatures. The two most common types of hydrate structures that form from natural gas/water systems are structure I and structure II hydrates. Structure I tends to enclathrate smaller natural gas molecules such as methane, whereas structure II tends to enclathrate larger natural gas molecules such as propane [20]. Hydrates nucleation is highly stoichastic and many hundreds of experiments must be performed in order to collect reliable statistics [19], [21].

Since hydrates are a multicomponent system, it is important to include the energy associated with the change in chemical potential as guest molecules are removed from the solution and concentrated in the new phase, when calculating the free energy of the nucleus [22]. In addition, the composition of the hydrate nucleus may be significantly different to the bulk which is formed nearer the three phase equilibrium line [22].

One of the first models for hydrate nucleation was proposed by Sloan and Fleyfel in 1991 [23] and is termed the Labile Cluster Hypothesis. In this model, hydrate nucleation occurs in three steps:

1. Clusters form spontaneously when a hydrophobic solute is dissolved in water in temperature, pressure and chemical potential conditions that are thermodynamically favourable for hydrates
2. Several of these clusters which contain one gas molecule and 20-24 water molecules associate to form a nucleus
3. Many such nuclei will form with different configurations but only one represents the stable hydrate structure and will continue to grow

Chemical reactions were proposed for each of the steps. The rate constants were fit to experimental data but had no molecular basis. A similar model [24] has since been proposed by Kvamme for nucleation at the gas-liquid interface. Recently as molecular dynamics and Monte Carlo simulations have become more readily available, the Labile Cluster Hypothesis has been heavily criticised. In addition, laboratory data using Neutron Diffraction and Differential Scanning Calorimetry [25] have shown that the hydrated shell around methane is approximately 1 Å larger in the hydrate phase compared to in solution and that the shell becomes more disordered during formation than either in solution or in the hydrate phase, indicating significant changes to the hydration shell. It is now believed that labile clusters only form easily in dilute solutions and that the energy barrier is huge for these clusters to agglomerate to a critical sized nucleus [8].

Nucleation phenomena for simplified first order phase transitions have been extensively studied using Ising models in two and three dimensions [29], [30]. it has been shown that such models combined with spectroscopic measurements [30] can be powerful in providing insights into nucleation phenomenon; it is now understood that the size of the critical nucleus will decrease as the quench depth is increased, tending towards zero at the spinodal [30]. Previously it was generally thought that the size of the critical nucleus would increase with quench depth, diverging at the spinodal.

In a paper by Radhakrishnan and Trout [8], Monte Carlo simulations of CO_2 hydrate nucleation were performed in an isothermal isobaric ensemble, with fixed bond angles, fixed bond lengths and with periodic boundary conditions [8]. Order parameters were formulated to characterise the spatial and orientational order of guest molecules Φ_i^{gg} and water molecules Φ_i^{hh} order in the system. The order parameters were based on the average geometrical distribution of the nearest neighbour bonds in the phases, and were used to calculate a free energy hyper surface using the Landau-Ginzburg theory. Nuclei of various sizes were implemented and the thermodynamic properties of these nuclei were measured using non-Boltzmann sampling. The size of the critical nucleus size was determined by analysing the free energy surface. For a liquid CO_2 and water system, the critical nucleus at the interface at 220K and 4 MPa was found to be between 9.6 and 14.5 Å which is significantly smaller than the 32 Å predicted by classical nucleation theory for a 7 K subcooling [12]. The implicit assumptions in this approach were that the size of system in the simulations does not affect the free energy barrier to nucleation, nucleation is governed by equilibrium thermodynamics, and that the set of order parameters chosen is complete in that the minimum free energy path to nucleation lies within the chosen order parameter space [8]. Transition path sampling [26], [27] would be a more rigorous approach to modelling nucleation and would allow these assumptions to be relaxed.

COMPUTER SIMULATION

Introduction

A two dimensional Ising model was constructed in Visual Basic to simulate nucleation and derive thermodynamic parameters for nuclei as a function of size. The system was represented as a discretised grid

with a user defined size of between 2 and 500 spaces. The new phase was denoted by the number 1 and the old phase by zero. A Monte Carlo approach was used for moving between configurations: a grid point was chosen at random and the phase inverted. The Metropolis algorithm was implemented to determine whether to accept or reject the new configuration.

Details of the Model

In order to allow the calculations to focus on a single nucleus, a second grid was defined within the original grid. This grid included all the cells within the nucleus and those immediately adjacent to it in the horizontal and vertical direction. The Monte Carlo method used to pick the cells to invert was then limited to this new grid. This modification was found to be necessary to prevent secondary nuclei from forming which would bias the statistics.

Problems were encountered with sampling the initial stage of nucleus formation and growth since Boltzmann sampling rapidly progresses to lower energy states that correspond to total conversion of the old phase to the new phase. These problems were overcome by implementing Window Sampling [31]. In this approach the nucleus is artificially forced to have a volume (or cross sectional area in two dimensions) between specified values. If the system attempts to move outside of this region the change will be rejected and the system reset to the previous conditions. The system will still spend significantly more time in the lower energy sections of the window, however random fluctuations will allow reasonable statistics to be collected for the higher energy sections within an acceptable timescale.

At the start of the simulation all of the grid points are set to a value of zero, a nucleus is then artificially introduced of a suitable size and shape. The algorithm is then initiated and the system is allowed to reach equilibrium. The number of time steps required for equilibrium to be reached was a function of the nucleus size and was defined for each run independently by performing a trial run and looking at how the shape of the nucleus changed, and looking at the data collected. Equilibrium was defined as the point when the distribution between the states no longer depends on run time. For the subsequent runs on that window, data was collected after the time steps had exceeded that required for equilibration.

Analysis of Results

The data for each window were then compiled. For each window, the integral of the probability of a volume (Vi) with volume equals unity. This leads to a scaling error between adjacent windows and discontinuities at the window boundaries. The source of this error is that the probability that the system is in one window or another is not accounted for in the model. In order to get the real probability of a volume (Vi), each of the probabilities from the window sapling method must be multiplied by the probability of the system being in that window.

Taking the natural log of the probabilities from the model reduces this multiplicative error to an additive error. The vertical positions of the lines can hence be adjusted by a constant so that there is no discontinuity at the window boundaries. The modified graph should then be converted back to a probability graph and normalised so that the integral equals unity.

Results and Discussion

Simulations were performed in a canonical ensemble (constant T,V and N) with a grid size of 30 by 30 with periodic boundary conditions. An external field of 2 J was applied and the grid points were all initially set to zero. It was decided to analyse the thermodynamic properties of nuclei with between 1 and 62 spins. The system was divided into 13 windows to allow efficient sampling. A Nucleus of a suitable size was introduced into the simulation for each window, the system was allowed to reach equilibrium for 100 steps and statistical measurements were then taken for a further 2000 steps.

After several attempts it became clear that nuclei of certain shape reached equilibrium faster than others. Perfectly rectangular nuclei took much longer to break free from that state due to the high energy cost obtained associated with increasing the surface area at the phase interface. The experiments were repeated with initial nuclei where the corners had been cut off. The 2000 step sampling time was chosen from experience since the shape of the distribution did not change after this point. In reality not all of the possible configurations will have been explored at this point, in particular the rectangular configuration had not been explored at all, otherwise the system would have got stuck there and the distribution of the statistics would have been poor. Ideally the system should have been allowed to sample statistics for several million steps in order to get good statistics for all configurations but my laptop can't cope with that.

When the probabilities of each configuration had been collected for each window they were converted to free energy and then corrected for the offset between the windows. The resulting chart is shown in Figure 2. The plot of the normalised probability is shown in Figure 3. The raw and processed data is presented in Appendix A. The location of the maximum in free energy corresponds to the maximum energy Ev shown in Appendix C.

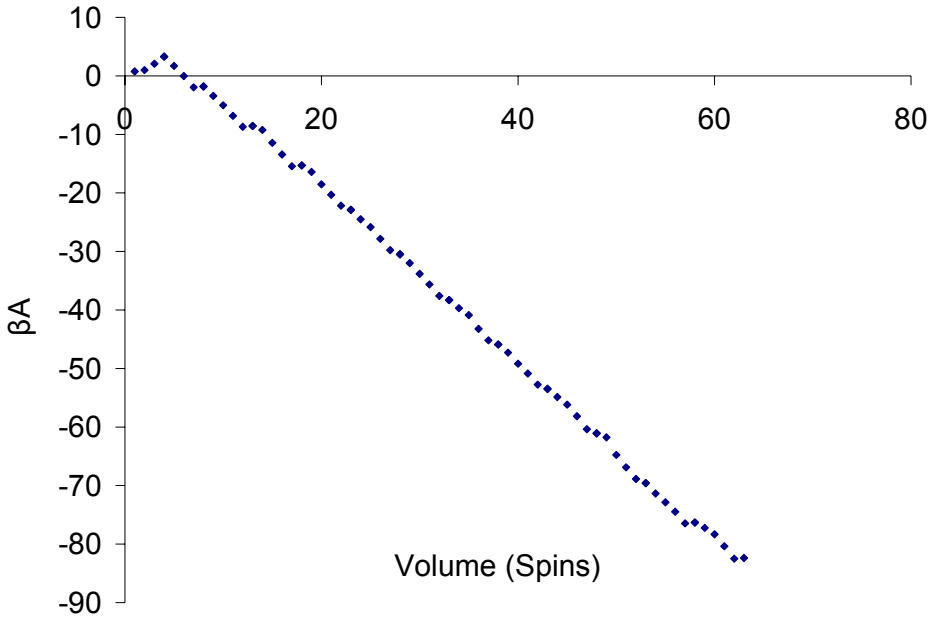

Figure 2: *Free Energy Plot for Nucleation in a Field of H=2 J and a Temperature of β=0.01 J from Window Sampling*

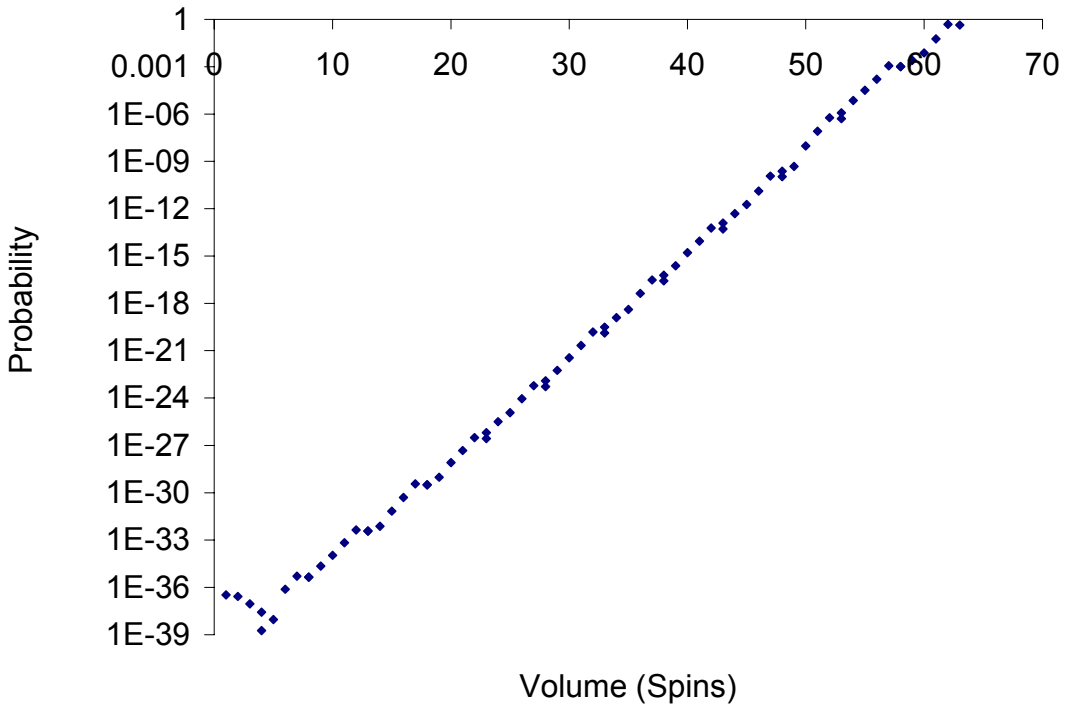

Figure 3: *Probability Plot for Nucleation in a Field of H=2 J and a Temperature of β=0.01 J from Window Sampling*

CONCLUSIONS

Predicting the onset of hydrate nucleation in oil pipelines is one of the most challenging aspects in the flow assurance modelling work being performed at the Center for Hydrate Research. Hydrate nucleation is a multicomponent phenomenon and any expression for the free energy of a nucleus must include contributions from the change of chemical potential of dissolved guest molecules. In addition many quasi-stable hydrate structures may be possible during formation of a critical nucleus which would lower the free energy path for nucleation. Hydrate nucleation in oil pipelines is unlikely to be homogeneous; the presence of solid materials such as reservoir sand, drilling cuttings, corrosion products and reservoir fracturing materials, and surfactants such as asphaltines and corrosion inhibitors may help to catalyse the formation of hydrates. The prediction of the effects and interactions between these effects, on the nucleation rate of hydrates in an industrially realistic system is beyond the scope of this project.

In this report, a simplified nucleation model was designed based on a two dimensional Ising model, in order to determine thermodynamic properties for nuclei of various sizes in a one-component homogeneously nucleating system. The model used the Monte Carlo algorithm to select the next state to be sampled. Window sampling was successfully applied to collect high resolution statistics for the high energy states around the energy barrier. It was demonstrated that the shape and height of the energy barrier can be determined for a nucleating system in this way.

Future work should focus on converting the two dimensional model to three dimensions. Heterogeneous nucleation could be investigated by studying the interaction of the new phase with artificial substrates with intermediate spin moments. The depletion of guest molecules in the surrounding fluid could be incorporated by introducing a new variable for each grid space to represent the concentration of the guest molecule, Fickian diffusion between adjacent cells could be assumed.

REFERENCES

[1] Oxtoby D.W. *Nucleation of First-Order Phase Transitions.* Accounts of Chemical Research. 1998, Vol. 31, p91-97.

[2] Khambaty S. and Larson M.A. *Crystal Regeneration and Growth of Small Crystals in Contact Nucleation.* I&EC Fundamentals. 1978, 17, p160.

[3] Larson M.A. *Solute Clustering and Secondary Nucleation.* Conference on Advances in Industrial Crystallization. 1990, College of Engineering Iowa State University. Preprint 91130.

[4] Bendig L.L. and Larson M.A. *Nuclei Generation from Repetitive Contacting.* AIChE Symposium Series. 1976, 25, p57.

[5] Becker D. and Döring W. *The kinetic treatment of nuclear formation in supersaturated vapors.* Annalen der Physik. 1935, Vol. 24, p719-52.

[6] Volmer M. and Weber A. Keimbildung in übersättigten Gebilden. Z. Phys. Chem. 1925, Vol. 119, p277.

[7] Xu D. and Johnson W.L. *Geometric Model for the Critical-Value Problem of Nucleation Phenomena Containing the Size Effect of Nucleating Agent.* Physical Review B. 2005, Vol. 72, Brief Reports 052101, 1-4.

[8] Radhakrishnan R. and Trout B.L. *A New Approach for Studying Nucleation Phenomena using Molecular Simulations: Application to CO_2 Hydrate Clathrates.* Journal of Chemical Physics. 2002, Vol. 117(4), p1786-1796.

[9] Hadjiagapiou I.A., Malakis A. and Martinos S.S. *Inverse-Range Parameter Dependence of Gas-Liquid Nucleation in a Yukawa Fluid: A Density Functional Approach.* Materials Science – Poland. 2005, Vol. 23(4), p891-897.

[10] Weeks J.D., Chandler D. and Andersen H.C. *Role of Repulsive Forces in Determining the Equilibrium Structure of Simple Liquids.* Journal of Chemical Physics. 1971, Vol. 54(12), p5237-5247.

[11] Oxtoby D.W. and Evans R. *Nonclassical Nucleation Theory for the Gas-Liquid Transition.* Journal of Chemical Physics. 1988, Vol. 89(12), p7521-7530.

[12] Larson M.A. and Garside J. *Solute Clustering and Interfacial Tension.* Journal of Crystal Growth. 1986, Vol. 76, p88-92.

[13] Tolman R.C. *The Effect of Droplet Size on Surface Tension.* Journal of Chemical Physics. 1949, Vol. 17(3), p333.

[14] Wood G.R. and Walton A.G. *Homogeneous Nucleation Kinetics of Ice from Water.* Journal of Applied Physics. 1970, Vol. 41(7), p3027-3036.

[15] Zeng X.C. and Oxtoby D.W. *Gas-Liquid Nucleation in Lennard-Jones Fluids.* Journal of Chemical Physics. 1991, Vol. 94(6), p4472-4478.

[16] Haymet A.D.J. and Oxtoby D.W. *A molecular theory for the solid–liquid interface.* Journal of Chemical Physics. 1981, Vol. 74(4), p2559-2565.

[17] ten Wolde P.R., Ruiz-Montero M.J. and Frenkel D. *Numerical Evidence for bcc Ordering at the Surface of a Critical fcc Nucleus.* Physical Review Letters. 1995, Vol. 75(14), p2714-2717.

[18] Popovitz-Biro R. et al *Induced Freezing of Supercooled Water into Ice by Self-Assembled Crystalline Monolayers of Amphiphilic Alcohols at the Air-Water Interface.* Journal of the American Chemical Society. 1994, Vol. 116, p1179-1191.

[19] Heneghan A.F. and Haymet A.D.J. *Liquid-to-Crystal Nucleation: A New Generation Lag-Time Apparatus.* Journal of Chemical Physics. 2002, Vol. 117(11), p5319-5327.

[20] Sloan E.D. *Clathrate Hydrates of Natural Gasses.* 2nd Edition. 1998, Marcel Dekker Inc. New York. P65-158.

[21] Heneghan A.F. et al. *Liquid-to-Crystal Nucleation: Automated Lag-Time Apparatus to Study Supercooled Liquids.* Journal of Chemical Physics. 2001, Vol. 115(16), p7599-7608.

[22] Anklam M.R. and Firoozabadi A. *Driving Force and Composition for the Multicomponent Gas Hydrate Nucleation from Supersaturated Aqueous Solutions.* Journal of Chemical Physics. 2004, Vol. 121(23), p11867-11875.

[23] Sloan E.D. and Fleyfel F. *A Molecular Mechanism for Gas Hydrate Nucleation from Ice.* AIChE Journal. 1991, Vol. 37(9), p1281-1292.

[24] Kvamme B. *A Unified Nucleation Theory for the Kinetics of Hydrate Formation.* Annals of the New York Academy of Science. 2000, Vol. 912, Gas Hydrates, p496-501.

[25] Koh C.A. et al. *Mechanisms of Gas Hydrate Formation and Inhibition.* Fluid Phase Equilibria. 2002, Vol. 194-197, p143-151.

[26] Dellago C., Bolhuis P.G. and Chandler D. *Efficient Transition Path Sampling: Application to Lennard-Jones Cluster Rearrangements.* Journal of Chemical Physics. 1998, Vol. 108(22), p9236-9245.

[27] Dellago C., Bolhuis P.G., Csajka F.S. and Chandler D. *Transition Path Sampling and the Calculation of Rate Constants.* Journal of Chemical Physics. 1998, Vol. 108(5), p1964-1977.

[28] Chandler D. *Introduction to Modern Statistical Mechanics.* Ist Edition. 1987, Oxford. P172-175.

[29] Pan A.C. and Chandler D. *Dynamics of Nucleatino in the Ising Model.* Journal of Physical Chemistry B. 2004, Vol. 108, p19681-19686.

[30] Pan A.C., Rappl T.J., Chandler D. and Balsara N.P. *Neutron Scattering and Monte Carlo Determination of the Variation of the Critical Nucleus Size with Quench Depth.* Journal of Physical Chemistry B. 2006, Vol. 110, p3692-3696.

[31] Chandler D. *Introduction to Modern Statistical Mechanics.* 1st Edition. 1987, Oxford. P172-174.

Appendix A: Raw and Processed Data:

Window	Spin	Frequency	Probability	βA	Adjusted βA	Adjusted P	Adjusted βA
1 to 4	1	915	0.462822458	0.77041176	0.770411758	3.34589E-37	83.98791704
	2	739	0.373798685	0.9840379	0.984037902	2.70231E-37	84.20154318
	3	250	0.126454224	2.06787491	2.067874905	9.14176E-38	85.28538018
	4	73	0.036924633	3.29887638	3.298876382	2.6694E-38	86.51638166
4 to 8	4	5	0.002530364	5.97939197	3.298876382	1.82928E-39	89.19689724
	5	25	0.012651822	4.36995405	1.68943847	9.14639E-39	87.58745933
	6	141	0.071356275	2.64006999	-0.040445596	7.52769E-37	83.17705968
	7	964	0.487854251	0.71773858	-1.962777	5.14659E-36	81.25472828
	8	841	0.425607287	0.85423822	-1.826277366	4.48992E-36	81.39122791
8 to 14	8	1	0.000506073	7.58882988	-1.826277366	4.48992E-36	81.39122791
	9	5	0.002530364	5.97939197	-3.435715278	2.24496E-35	79.78179
	10	24	0.012145749	4.41077605	-5.004331196	1.07758E-34	78.21317408
	11	147	0.074392713	2.59839729	-6.816709952	6.60019E-34	76.40079533
	12	964	0.487854251	0.71773858	-8.69736866	4.32829E-33	74.52013662
	13	835	0.42257085	0.86139815	-8.55370909	3.74909E-33	74.66379619
13 to 18	13	1	0.000506073	7.58882988	-8.55370909	3.74909E-33	74.66379619
	14	2	0.001012146	6.8956827	-9.246856271	7.49817E-33	73.97064901
	15	18	0.009109312	4.69845812	-11.44408085	6.74835E-32	71.77342443
	16	132	0.066801619	2.70602796	-13.43651101	4.94879E-31	69.78099427
	17	970	0.490890688	0.71153381	-15.43100516	3.63661E-30	67.78650012
	18	853	0.431680162	0.84007033	-15.30246864	3.19797E-30	67.91503664
18 to 23	18	1	0.000505817	7.58933582	-15.30246864	3.19797E-30	67.91503664
	19	3	0.001517451	6.49072353	-16.40108093	9.59391E-30	66.81642435
	20	25	0.012645422	4.37046	-18.52134446	7.99492E-29	64.69616082
	21	148	0.0748609	2.59212355	-20.29968091	4.733E-28	62.91782437
	22	963	0.487101669	0.71928241	-22.17252205	3.07964E-27	61.04498323
	23	837	0.423368741		-22.89180446	2.6767E-27	61.18521257
23 to 28	23	1	0.000505817	7.58933582	-22.89180446	6.32239E-27	60.32570082
	24	5	0.002529084	5.97989791	-24.50124237	3.16119E-26	58.7162629
	25	19	0.009610521	4.64489684	-25.83624344	1.20125E-25	57.38126184
	26	142	0.071825999	2.63350877	-27.84763152	8.97779E-25	55.36987376
	27	970	0.490642387	0.71203975	-29.76910053	6.13271E-24	53.44840475
	28	840	0.424886191		-30.48114028	5.3108E-24	53.59229893
28 to 33	28	2	0.000401929	7.81923445	-30.48114028	1.24994E-23	52.73636499
	29	9	0.001808682	6.31515706	-31.98521768	5.62471E-23	51.2322876
	30	56	0.011254019	4.48702994	-33.81334479	3.49982E-22	49.40416048
	31	345	0.069332797	2.66883722	-35.63153752	2.15614E-21	47.58596776
	32	2431	0.488545016	0.71632366	-37.58405108	1.5193E-20	45.6334542
	33	2133	0.428657556		-38.30037474	1.33306E-20	45.76422746
33 to 38	33	1	0.000506329	7.58832368	-38.30037474	3.10984E-20	44.91713054
	34	4	0.002025316	6.20202932	-39.6866691	1.24394E-19	43.53083618
	35	13	0.006582278	5.02337432	-40.8653241	4.04279E-19	42.35218118
	36	138	0.069873418	2.66106999	-43.22762842	4.29158E-18	39.98987685
	37	974	0.493164557	0.70691237	-45.18178604	3.02898E-17	38.03571924
	38	845	0.427848101		-45.88869842	2.62781E-17	38.17779391
38 to 43	38	1	0.000506073	7.58882988	-45.88869842	6.14193E-17	37.32880686
	39	4	0.002024291	6.20253552	-47.27499278	2.45677E-16	35.9425125
	40	27	0.013663968	4.29299301	-49.18453528	1.65832E-15	34.03297
	41	143	0.072368421	2.62598525	-50.85154305	8.78297E-15	32.36596223
	42	960	0.48582996	0.72189659	-52.7556317	5.89626E-14	30.46187358
	43	841	0.425607287		-53.47752829	5.16537E-14	30.5942152
43 to 48	43	1	0.000506073	7.58882988	-53.47752829	1.21365E-13	29.73997698
	44	4	0.002024291	6.20253552	-54.86382265	4.85458E-13	28.35368262
	45	15	0.007591093	4.88077968	-56.18557849	1.82047E-12	27.03192678
	46	108	0.05465587	2.90669865	-58.15965952	1.31074E-11	25.05784576
	47	973	0.492408907	0.7084458	-60.35791238	1.18088E-10	22.8595929
	48	875	0.442813765		-61.06635817	1.06194E-10	22.9657531
48 to 53	48	1	0.000200924	8.51258258	-61.06635817	2.39816E-10	22.15114711
	49	2	0.000401849	7.8194354	-61.75950535	4.79633E-10	21.45799993
	50	40	0.00803697	4.82370312	-64.75523763	9.59266E-09	18.46226765
	51	338	0.067912397	2.68953668	-66.88940407	8.1058E-08	16.32810121
	52	2448	0.491862568	0.70955594	-68.86938482	5.87071E-07	14.34812046
	53	2148	0.431585292		-69.57894075	5.15126E-07	14.47885465
53 to 58	53	1	0.000506073	7.58882988	-69.57894075	1.19357E-06	13.63856453
	54	6	0.003036437	5.79707041	-71.37070022	7.1614E-06	11.84680506
	55	27	0.013663968	4.29299301	-72.87477762	3.22263E-05	10.34272766
	56	135	0.068319838	2.6835551	-74.48421553	0.000161132	8.733289749
	57	961	0.486336032	0.72085547	-76.44691516	0.001147018	6.770590118
	58	846	0.428137652	0.84831052	-76.31946011	0.001009757	6.898045168
58 to 63	58	2	0.001012146	6.8956827	-76.31946011	0.001009757	6.898045168
	59	5	0.002530364	5.97939197	-77.23575084	0.002524394	5.981754436
	60	15	0.007591093	4.88077968	-78.33436313	0.007573181	4.883142147
	61	116	0.058704453	2.83523969	-80.37990312	0.05856593	2.837602157
	62	971	0.491396761	0.71050341	-82.5046394	0.490237221	0.71286588
	63	867	0.438765182	0.8237909	-82.39135191	0.437729836	0.826153372

Appendix B: Visual Basic Code

Appendix C: Measured Properties from Simulations